DOI: 10.13009/EUCASS2017-432



# Vortex-Sound Modelling in Aft-Finocyl Solid Rocket Motors

*G. Rossi*⋆†, *M. Laureti*⋆, *B. Favini*⋆, *E. Cavallini*∗ *and A. Neri*⋆⋆
⋆*Sapienza University of Rome - Dept. of Mechanical and Aerospace Engineering*
*Via Eudossiana 18 - 00184, Rome, Italy*
giacomo.rossi@uniroma1.it · mariasole.laureti@uniroma1.it · bernardo.favini@uniroma1.it
∗*Italian Space Agency ASI - Scientific Research Division*
*Via del Politecnico snc - 00133, Rome, Italy*
enrico.cavallini@asi.it
⋆⋆*European Space Agency - ESRIN Integrated Project Team*
*Via Galileo Galilei - 00044, Frascati (Rome), Italy*
agostino.neri@esa.int
†Corresponding author

## Abstract

This paper has the aim to investigate the correlation between some ballistic geometrical parameters of a SRM and the calibration of AGAR Q1D model of the pressure oscillations. The correlation permits to share the same model calibration between SRMs of different scales prone to pressure during their steady state, improving the prediction capability of the model. The numerical reconstructions performed on two aft-finocyl SRMs, P80 the first stage of the European launch vehicle VEGA, and POD-Y the mid-scale demonstrator for the pressure oscillations of the possible future evolutions of P80 SRM, confirm the effectiveness of this approach and the goodness of the AGAR model, both numerical results being in very good agreement with experimental data.

## 1. Introduction

The operative life of many large solid rocket motors (e.g. US Space Shuttle SRM, Titan SRM and the five-segment test motor ETM-3,[1–3] Ariane 5 P230 SRM[4] and P80 SRM[5]) is characterized by the presence of sustained longitudinal pressure and thrust oscillations during their steady state. Segmented SRMs and monolithic finocyl SRMs are prone to pressure oscillations phenomena, with different characteristics time windows: during the second half of the SRM functioning, for the segmented SRMs; during the first half of the operative life, for the aft-finocyl configurations. The frequency of the pressure oscillations (PO) is close to the first, but sometimes also to higher longitudinal acoustic frequencies of the combustion chamber. Although they do not compromise the motor life, such oscillations may represent an important issue, which has to be accounted for at the system level. Their occurrence has to be carefully evaluated in order to correctly assess the pressure oscillations time windows and amplitude which represents an input for the structures dimensioning, above all, for the stage interfaces, equipment and the payload adapter, in order to correctly characterize the dynamic environment. In fact, pressure oscillations of the order of about 0.5 % of the mean value, due to the transfer function between pressure and thrust, can generate thrust oscillations about 5 % of the mean thrust value.

The pressure oscillation phenomenon[6,7] is one of the effect of the very complex flowfield that develops in the combustion chamber of SRMs: the propellant grain typically consist of a mixture of granules of solid oxidizer (ammonium nitrate, ammonium perchlorate, potassium nitrate) in a polymer binder (binding agent) with flakes or powders of energetic compounds (RDX, HMX), and/or metallic additives (Aluminium, Beryllium), plasticizers, stabilizers, and/or burn rate modifiers (iron oxide, copper oxide). Because of the presence of this multicomponent mixture, the combustion of the propellant surface is highly not-homogeneous. The first effect of this inhomogeneity is that the flame front affects vorticity generation but also the vortex shedding phenomenon, generated by the abrupt port area variation, as grain segmentation or aft-finocyl configuration. Another effect is that into the gas phase are dispersed solid burning particles, typically of alumina or uncombusted aluminium, that release a significant amount of heat into the flux, affecting the fluctuating nature of the flowfield.

Both P80, the first stage of VEGA launcher and POD-Y,[8,9] the demonstrator of large/intermediate scale aft finocyl SRMs have experimentally shown the presence of sustained pressure oscillation at the first longitudinal mode

DOI: 10.13009/EUCASS2017-432



of the combustion chamber during the steady-state. The main difference between these SRMs is the amplitude of this oscillation, that scales roughly proportional with the motor scale (P80 SRM is more than three times bigger than the POD-Y SRM)[10]. The amount of experimental data available is also very different: for the P80 SRM, the SFTs performed during the VEGA development phase (P80 DM and P80 QM), and the VEGA flights represent a wide experimental evidence of the SRMs behaviour with respect to the pressure oscillation phenomena. Instead, for the POD-Y, only one SFT has been performed on March 2015, as per the experimental data reported in,[8] not allowing a characterization of the dispersion of the pressure oscillations occurrence for such kind of SRM. In figure 1a are reported some experimental data for P80 SRM;[11] the pressure oscillations appear to be repetitive among the SFTs and the flights (only VV01 and VV02): four different blows, named B0, B1, B2 and B3 are clearly present both for SFT and the flights. The first blow occurs immediately after the SRM start-up and has not a well definite time window; the second blow (B1) is the most repetitive among all the firings, in terms of both the maximum amplitude and window of occurrence; the third blow (B2) presents a time window of occurrence with a high dispersion for its starting time and a very low dispersion for the ending time, unlike the fourth blow (B3), that presents a starting time almost constant and ending times not so close between all the firings. The frequency content for all the blows is organized at the 1L mode of the P80 combustion chamber, without almost any involvement of organized oscillations at higher longitudinal fundamental modes.

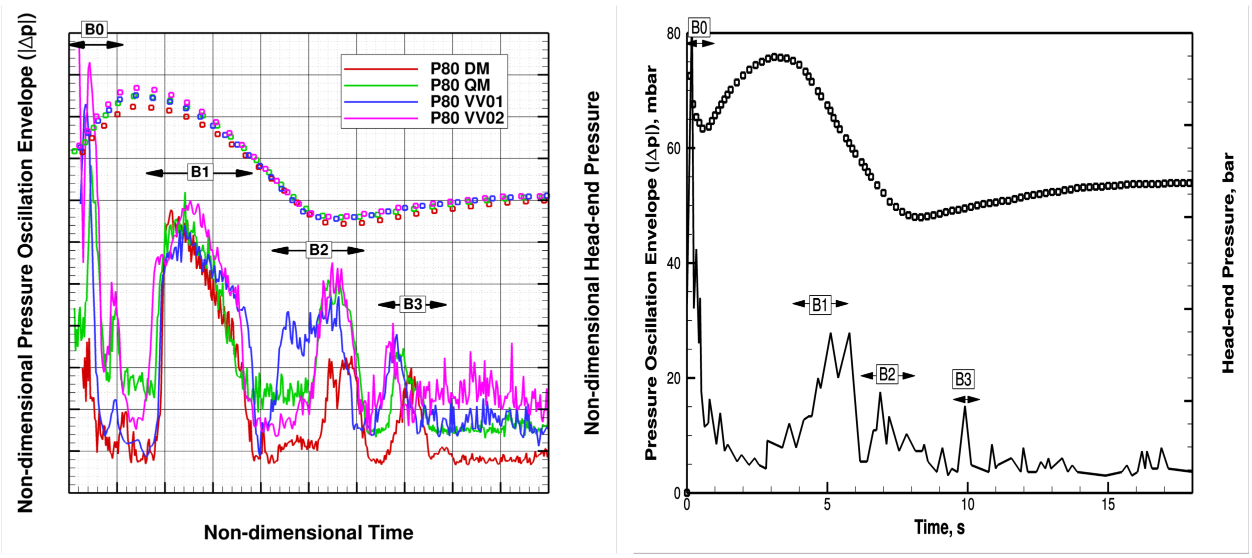


(a) P80[11]

(b) POD-Y[8]

Figure 1: P80 and POD-Y Head pressure and pressure oscillations evolution in time (half of combustion time)

In figure 1b are reported the experimental data for the only one SFT of POD-Y: four blows are present, and the time window of occurrence seems very similar to the P80 blows, also if, as already underlined, the only one SFT doesn't permit a complete characterization of the PO phenomena for this SRM. Also in this case, only the 1L mode of the SRM is involved in the pressure oscillations.[8]

From the analysis of the experimental data some similarities between the PO of the two SRMs can be highlighted. The first blow appears immediately after the ignition transient and lasts for a small time with respect to the overall SRM combustion time. The second blow occurs immediately after the reaching of the motor operating maximum pressure and lasts up to a phase where the submergence region is going to burn-out, emptying itself of propellant grain. Both of these blows, moreover, are characterized by a propellant grain configuration with a relevant mass addition from the aft-star-shaped region of the propellant grain, which is burnt-out afterwards. The third and fourth blows occur after the head end pressure curve knee, in a phase where the aft-part of the SRM is completely burnt-out.

The differences in the amplitude and time-windows of the pressure oscillations of the P80 and of the POD-Y SRMs (which are more than one order of magnitude higher for the P80 in comparison to the POD-Y), are not justified only by the different sizes of the two SRMs, highlighting that, even if a scale effect can be present, the SRM internal geometry has to play a relevant role in the feedback loop between vortical structure generation and acoustic mode excitation.[10] This statement is also supported by the experimental evidences of other aft-finocyl SRMs, Zefiro 16 (technology demonstrator of VEGA SRMs), Z23 SRM (second stage of VEGA) and Z9 SRM (third stage of VEGA), which even being of different size, comparable with the POD-Y one, do not suffer of any pressure oscillation phenomena.

DOI: 10.13009/EUCASS2017-432



This paper discusses the numerical reconstruction of pressure oscillations for the aft-finocyl SRMs, P80 and POD-Y, within a framework of simulation already presented in the recent past,[10–14] based on a Q1D modelling of the pressure oscillations phenomena of SRMs, named AGAR. The purpose is to investigate the correlation of one of the model parameters of the AGAR, that will be presented in sec. 2 with the SRM ballistic and geometrical quantities, in order to provide a theoretical-based rationale of the model set-up for SRM with different sizes, geometrical configuration and pressure oscillations amplitude, to investigate the chance to apply the same model to new SRMs without any fine calibration of the model set-up.

## 2. Internal Ballistics Q1D Model of SRMs Acoustic Resonance

The model developed for the pressure oscillations simulation during the SRM internal ballistics, named AGAR (Aerodynamically Generated Acoustic Resonance) is composed by the following three models: a model of the SRM internal ballistics (SPINBALL - Solid Propellant rocket motor INternal BALListics,[15–17] which is based on a one-phase unsteady quasi-one-dimensional Eulerian formulation of the SRM flowfield, with mass, momentum and energy addition, that accounts for the evolution in time of the SRM geometrical configuration); a model for the grain burnback simulation (GREG - Grain REGression, based on a level set technique properly tailored to the evolution of the combustion surface of the SRMs); an aeroacoustic model (POX - Pressure Oscillation). It is important to underline that, the model itself doesn't distinguish the two different contributions leading to the onset of the pressure oscillations - lock-in between the longitudinal acoustic modes / vorticity dynamic, parietal flame and distributed combustion dynamic and their sound-generation - being the variable that here is called vorticity actually a more general "vortex plus solid phase burning".

The aeroacoustic model is composed by the following sub-models: a model to determine the vorticity dynamics (creation, growth, convection and destruction), a model to evaluate the acoustic field excitation by vorticity (vortex-sound generation), and a model to estimate the acoustically forced vorticity generation. A Q1D equation describes the vorticity convection in the flow. The acoustic modes excitation due to vorticity impingement is modelled with the introduction of source terms in the Q1D unsteady gasdynamic model. In a Q1D model, only the azimuthal component of the vorticity, concurrently orthogonal to the motor axial and radial directions, has to be modelled. The model is formally derived from from the multi-dimensional vorticity equation in cylindrical coordinates and after the assumptions of axisymmetric flow ( $u_\theta = (\cdot)_\theta = 0$), the conservative form of the resultant equation is averaged over the section; more details can be found in previous works.[11,13]

Source terms are added to the standard set of Q1D Euler equations to describe the vortex-sound generation. These terms represent the acoustic excitement of the flowfield due to POX interaction/impingement with obstacles and or, in general, the combustion chamber geometry after the POX detachment itself. The expressions introduced to model the source terms derive from taking into account the decomposition of convective flux into the momentum equation on the basis of the D'Alambert identity. By so doing the POX-sound terms are enucleated and heuristically modelled in the form reported in Eq. (1).

$$
\begin{cases}
\dfrac{\partial\left(\rho A_p\right)}{\partial t} + \dfrac{\partial\left(\rho u\, A_p\right)}{\partial x} = r_b P_b \rho_p + \dfrac{\dot{m}_s A_p}{V} + \dfrac{\dot{m}_{ig} A_p}{V} \\
\dfrac{\partial\left(\rho u A_p\right)}{\partial t} + \dfrac{\partial\left[\left(\rho u^2 + p\right) A_p\right]}{\partial x} - p\dfrac{\partial A_p}{\partial x} = \dfrac{\dot{m}_{ig} A_p \bar{v}_{inj}}{V} + \dfrac{1}{2}\rho u^2 c_f + \underbrace{\rho\, \omega a \left(\dfrac{\partial A_p}{\partial x}\right) L}_{\text{vortex sound}} \\
\dfrac{\partial\left(\rho e A_p\right)}{\partial t} + \dfrac{\partial\left[\left(\rho e + p\right) u A_p\right]}{\partial x} = r_b P_b \rho_p H_f + \dfrac{\dot{m}_{ig} A_p H_{ig}}{V} + \dfrac{\dot{m}_s A_p H_s}{V} + \underbrace{\rho\, u\, \omega a \left(\dfrac{\partial A_p}{\partial x}\right) L}_{\text{vortex sound}} \\
\dfrac{\partial\left(\omega\, A_p\right)}{\partial t} + \dfrac{\partial\left(k_u\, u\, \omega A_p\right)}{\partial x} = k_\Gamma\, u^2
\end{cases}
\tag{1}
$$

Two calibration parameters are introduced in the model: $k_u$ and $k_\Gamma$: the first one is used to take into account that the Q1D model average flowfield overestimates the advection velocity of the POX in the flowfield (because of the mass addition and the rotation of the streamlines from the propellant surface towards the motor axis); the latter is used to model the amount of vorticity generated upstream the aft-finocyl region. These two parameters, since their different role in the model, have almost independent effects of the pressure oscillation results: the $k_u$ affects the lock-in condition and, therefore, the pressure oscillations time windows; whereas, the $k_\Gamma$ has effect on the level of the pressure oscillations, since it characterizes the intensity of vorticity generation inside the SRM, therefore vortex-sound if the lock-in condition occurs.

DOI: 10.13009/EUCASS2017-432



As far as the vortex characterization before its detachment in the flowfield is concerned, a detachment criterion is developed as a function of the time varying flow conditions. The criterion is the one already presented in Ref. 13 and considers the local pressure evolution at the shedding point, i.e. the detachment point of the geometry, defining again the role of the acoustic feedback on vortex shedding dynamics. The vortex separation is imposed each time the pressure evolution of the detachment point that is a descending node (which corresponds to a positive velocity anti-node).

### 2.1 $k_\Gamma$ Parameter Discussion

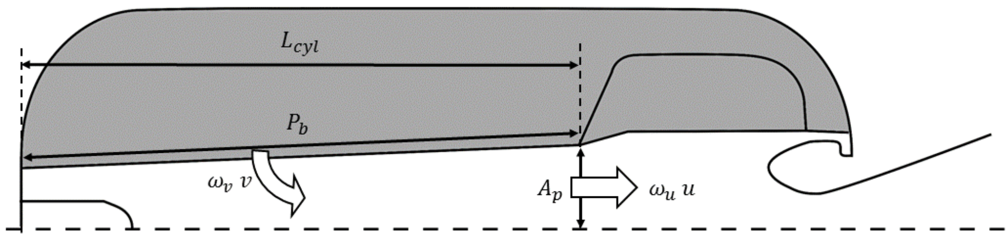


Figure 2: Sketch of vorticity balance and SRM geometrical quantities

The $k_\Gamma$ parameter represents the vorticity generation coefficient to model the vorticity generated upstream the aft-finocyl region: it mainly affects the pressure oscillation amplitude. To relate this parameter to SRM characteristics, let assume a steady flow of an ideal fluid; the balance of the vorticity flux injected upstream the finocyl transition and the vorticity flux issuing through the port area at the finocyl transition itself is:

$$\omega_v v P_b L_{cyl} = \omega_u u A_p \tag{2}$$

where, referring to figure 2, $A_p$ is the port area immediately upstream the finocyl transition, $L_{cyl}$ is the length of the cylindrical tapered grain upstream the finocyl transition region, $P_b$ is the average combustion perimeter in the cylindrical tapered region, $u$ is the axial average velocity at the entrance of the finocyl transition, $v$ is the injection velocity of the flow at wall, $\omega_u$ is the average vorticity at the entrance of the finocyl transition and $\omega_v$ is the average vorticity injected upstream the finocyl transition because of the turning flow and propellant grain combustion.

Assuming that $\omega_u = \alpha u$, Eq. (2) can be written as:

$$\omega_v v P_b = \alpha \frac{A_p}{L_{cyl}} u^2 \tag{3}$$

therefore, the parameter $k_\Gamma$ in system (1) can be written as:

$$k_\Gamma = \alpha \frac{A_p}{L_{cyl}} \tag{4}$$

showing that $k_\Gamma$ parameter is proportional to the ratio between the port area at the end of the cylinder section and the cylinder section length.

## 3. Numerical Simulations

### 3.1 P80 Numerical Simulation

In previous works[10,11] are reported the numerical simulation performed with AGAR framework on P80 SRM. The parameters $k_u$ and $k_\Gamma$ used in these simulations are evaluated from a reconstruction of the experimental data (figure 1a), with an average model set-up in terms of the two calibration parameters ($k_\Gamma$, $k_u$), considering the dispersion of the static firing tests (DM and QM) and flight data (VV01 and VV02).

Using the average calibration for both $k_\Gamma$ and $k_u$ parameters, the numerical simulation obtained (see figure 3a) shows very good agreement for time window of occurrence, amplitude and trend for B0 and B1 blows with respect to the experimental data. Concerning B2 and B3 blows, however, there are some differences with the SFT and flights data: the initial onset of the B2 is well captured, as its maximum amplitude, but the numerical simulation shows only one blow, instead of the two present in all the experimental data.

DOI: 10.13009/EUCASS2017-432



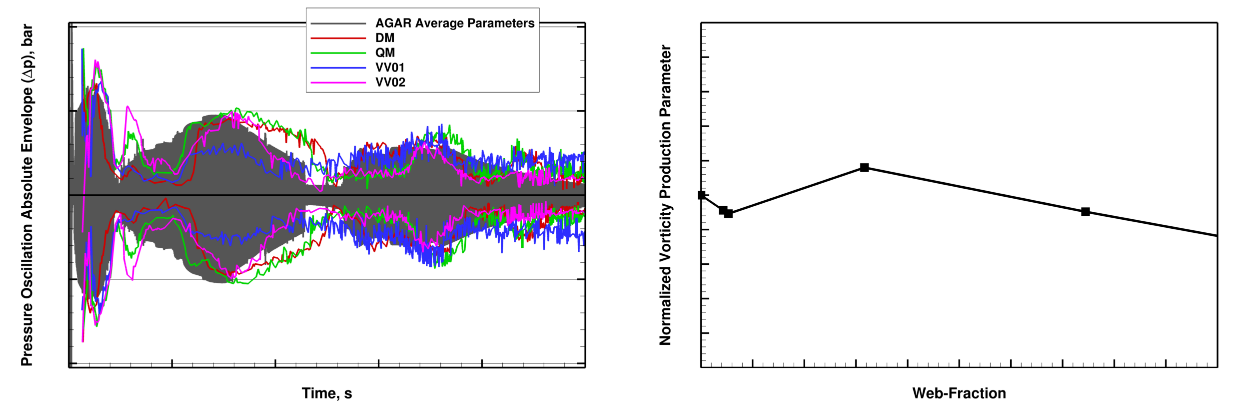


(a) AGAR P80 simulation with average $k_u$ and $k_\Gamma$ calibrations

(b) P80 $\alpha$ parameter

Figure 3: P80 numerical pressure oscillations reconstruction and $\alpha$ parameter (half of combustion time)

At the time of occurrence of the two last blows, indeed, the aft-finocyl propellant grain configuration is such that the submergence region is almost empty of residual mass propellant (and so the mass addiction from this SRM part is almost null), while at B0 and B1 time of occurrence the situation is reversed, and the submergence zone gives a large contribution to the mass addiction.

Once $k_\Gamma$ is obtained through the calibration of numerical solution with respect to experimental data, by means of Eq. (4) is possible to evaluate the POX production parameter as:

$$\alpha_{P80} = \frac{k_{\Gamma_{P80}}}{\left(\frac{A_p}{L_{cyl}}\right)_{P80}} \tag{5}$$

From the ratio between the $k_\Gamma$ of the average simulation shown in figure 3a and the ballistic parameter $A_p/L_{cyl}$ it is possible to obtain an $\alpha$ parameter trends, reported in figure 3b. The trend reported in figure 3b allow to make the following remarks: $\alpha$ parameter is almost constant, besides the different SRM blow level and the trend somewhere not continuous of $\alpha$ is due to the combination of a regular trend for the $A_p/L_{cyl}$ geometrical factor and the one of the $k_\Gamma$ parameter. The amount of P80 experimental data allows to have a strong and consolidated reconstruction of the $\alpha$ parameter.

### 3.2 POD-Y Numerical Simulation

Let us assume that $\alpha$ parameter could be constant whatever other SRM of aft-finocyl class are considered and in particular for the POD-Y SRM. Therefore the calibration parameter $k_\Gamma$ for the POD-Y SRM can be defined as:

$$k_{\Gamma_{POD-Y}} = \alpha_{P80} \left(\frac{A_p}{L_{cyl}}\right)_{POD-Y} \tag{6}$$

Figure 4 shows the comparison of the numerical simulation of POD-Y SRM with the $k_\Gamma$ evaluated from Eq. (6) and the experimental data, confirming that the assumption about the independence of the $\alpha$ parameter from the specific SRM appears correct at least in this case. Due to the only one SFT, is impossible to extract any information about the dispersion of the experimental data: in the numerical prediction, the first relevant blow, divided into two phases in the experimental data, is slightly underestimated in terms of pressure oscillation amplitude, and the time window of occurrence is slightly shifted forward. The numerical simulations show moreover, that only the 1L mode of the SRM is involved in the pressure oscillations, as indicated in the reference papers.[8,9] Some differences are present for the blow immediately after the ignition transient, that is however difficult to be reconstructed as start-up phase because the lack of information about the ignition device of the POD-Y SRM. The present numerical simulation has been obtained with a constant value of the $k_u$ parameter and the effect of $k_u$ variation in time will be considered in a forthcoming paper.

## 4. Conclusions

The AGAR model provides the numerical simulation of pressure oscillations in aft-finocyl SRMs with a Q1D model, which has been validated by means of the analysis of the pressure oscillations of two aft-finocyl SRMs with different

DOI: 10.13009/EUCASS2017-432



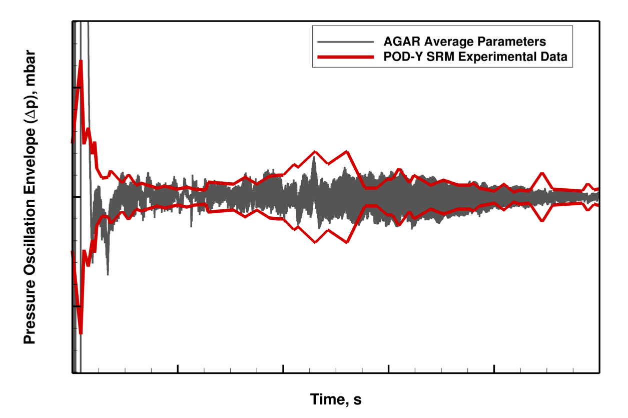


Figure 4: AGAR POD-Y simulation with average $k_u$ and $k_\Gamma$ calibrations (half of combustion time)

sizes: P80, first stage of the European launch vehicle VEGA and POD-Y SRM, mid-scale demonstrator for the pressure oscillations of the possible evolution of the P80 SRM. The experimental data of the two SRMs show that, besides the different sizes and geometrical configurations, similar characteristics of occurrence of the phenomenon are present: POs occur in the first half of the SRM functioning, involving only the 1L mode of the SRM combustion chamber. The mail difference between the POs of the two SRMs is, instead, represented by their amplitude, being the POD-Y one, roughly one order of magnitude lower that the P80 ones. Both numerical reconstructions of the pressure oscillations of P80 and POD-Y SRM are in very good agreement with the experimental data, leading to different model set-up.

AGAR model has, indeed, two calibration parameters: one is the correction coefficient for the vorticity flow advection with respect to the Q1D average velocity, which affects mainly the pressure oscillation time windows and another is the vorticity generation coefficient that models the amount of vorticity generated upstream the aft-finocyl region, mainly affecting the pressure oscillation amplitude.

This last model parameter can be related, via a simple vorticity balance between the whole cylindrical section and its end, to the $A_p/L_{cyl}$ geometrical factor, where $A_p$ is the port area at the end of the cylindrical section of aft-finocyl SRMs and $L_{cyl}$ the length of this cylindrical section. The relationship obtained allows to use the $k_\Gamma$ calibration parameter of one SRM to obtain the $k_\Gamma$ of another SRM via the geometrical factor ratio between the two SRMs.

The numerical simulation carried out with AGAR model on the POD-Y SRM shows that, using the relation between $k_\Gamma$ and $A_p/L_{cyl}$, is possible to achieve numerical results that are in very good agreement with experimental data, without any fine calibration on the model.

This activity represents a further step towards the investigations of the AGAR model capability in the simulation of the pressure oscillation phenomena of aft-finocyl SRM, and, in particular towards a robust and demonstrated prediction capability of the model in a wide range of aft-finocyl SRMs. Concerning this point, it is worth highlighting that for Zefiro 23 SRM and Zefiro 9 SRM, respectively second and third stage of VEGA launch vehicle, not prone at all to PO phenomena by experimental evidence, the AGAR model does not show any aero-acoustic coupling applying a wide range of the model set-up around the one considered for the P80/POD-Y SRMs, demonstrating that when a motor is not prone to pressure oscillations, the model does not provide them.

## Acknowledgements

This work is supported and funded by the ESA-ESRIN/Contract No. 4000101871/10/I/JD. All the required motor data of VEGA SRMs have been kindly granted by ESA ESRIN Integrated Project Team.

VEGA launch vehicle was developed within a European Program promoted by the European Space Agency (ESA), as a cooperative project with Member States within the ESA framework. VEGA Programme was been managed by an Integrated Project Team that, under the responsibility of the European Space Agency, involved also staff from the Italian (ASI) and French (CNES) Space Agencies.

The POD-Y was developed first under CNES funding and then under ESA Contract No. 4000108839/13/F/MT with Herakles (France).

DOI: 10.13009/EUCASS2017-432



## References

[1] Brown, R., Dunlap, R., Young, S., and Waugh, R., "Vortex shedding as a source of acoustic energy in segmented solid rockets," *Journal of Spacecraft and Rockets*, Vol. 18, No. 4, 1981, pp. 312–319.

[2] Dotson, K., Koshigoe, S., and Pace, K., "Vortex shedding in a large solid rocket motor without inhibitors at the segment interfaces," *Journal of Propulsion and Power*, Vol. 13, No. 2, 1997, pp. 197–206.

[3] Mason, D., Morstadt, R., Cannon, S., Gross, E., and Nielsen, D., "Pressure oscillations and structural vibrations in Space Shuttle RSRM and ETM-3 Motors," *AIAA Paper*, Vol. 3898, 2004.

[4] Scippa, S., Pascal, P., and Zanier, F., "Ariane 5-MPS - Chamber pressure oscillations full scale firing results: Analysis and further studies," *30th Joint Propulsion Conference and Exhibit*, Joint Propulsion Conferences, American Institute of Aeronautics and Astronautics, jun 1994.

[5] Cavallini, E., Paglia, F., and Favini, B., "Analysis & Reconstruction of Pressure Oscillations during P80 Steady-State of VEGA Flights," AIAA, July 2017, $5^{rd}$ AIAA/ASME/SAE/ASEE Joint Propulsion Conference and Exhibit, Atlanta, Georgia.

[6] Culick, F., "Acoustic oscillations in solid propellant rocket chambers," *Astronautica Acta*, Vol. 12, No. 2, 1966, pp. 113–126.

[7] Flandro, G., "Vortex driving mechanism in oscillatory rocket flows," *J. Propulsion and Power*, Vol. 2, No. 3, 1986, pp. 206–214.

[8] Larrieu, S., Godfroy, F., Orlandi, O., Robert, E., Ciucci, A., and Cesco, N., "Demonstration of Pressure Oscillation Reduction in the Frame of New Launchers Development," EUCASS, July 2015, $6^{th}$ European Conference for AeroSpace Sciences, Krakov.

[9] Larrieu, S., "Demonstration of Pressure Oscillation Reduction For a New Large Monolithic Motor," 2016, Paper n. 3125096, 2-6 May, Rome, Italy.

[10] Cavallini, E., Favini, B., and Neri, A., "Motor Scale and Propellant Geometry Effects on Pressure Oscillations in Aft-Finocyl Solid Rocket Motors," Propulsion and Energy Forum, American Institute of Aeronautics and Astronautics, July 2016, AIAA Paper 2016-4793, AIAA Propulsion & Energy Forum 2016, Salt Lake City, UT.

[11] Cavallini, E., Favini, B., and Neri, A., "Q1D Modelling of Vortex-Driven Pressure Oscillations in Aft-Finocyl SRMs with Submerged Nozzle Cavity," Propulsion and Energy Forum, American Institute of Aeronautics and Astronautics, July 2015, AIAA Paper 2015-3975, AIAA Propulsion & Energy Forum 2015, Cleveland, Florida.

[12] Ferretti, V., Favini, B., Cavallini, E., Serraglia, F., and Giacinto, M. D., "Numerical simulations of acoustic resonance of Solid Rocket Motor," AIAA-2010-6996, July 2010, 46th AIAA/ASME/SAE/ASEE Joint Propulsion Conference and Exhibit, Nashville, TN, July 25-28, 2010.

[13] Ferretti, V., Favini, B., Cavallini, E., Serraglia, F., and Giacinto, M. D., "Pressure oscillations simulation in P80 SRM first stage VEGA launcher," AIAA-2011-6055, July 2011, 47th AIAA/ASME/SAE/ASEE Joint Propulsion Conference and Exhibit, San Diego, California, July 31-3 August, 2011.

[14] Cavallini, E., Ferretti, V., Favini, B., Di Giacinto, M., and Serraglia, F., "Pressure Oscillations Numerical Simulation in Solid Rocket Motors," AIAA 2012-3824, August 2012, $48^{th}$ AIAA/ASME/SAE/ASEE Joint Propulsion Conference and Exhibit, 30 July - 1 August 2012, Atlanta, Georgia.

[15] Cavallini, E., Favini, B., Di Giacinto, M., and Serraglia, F., "Internal Ballistics Simulation of a NAWC Tactical SRM," *Journal of Applied Mechanics ISSN: 0021-8936; eISSN: 1528-9036*, , No. JAM-10-1424.

[16] Cavallini, E., Bianchi, D., Favini, B., Di Giacinto, M., and Serraglia, F., "Internal Ballistics Modeling of High Performance SRMs with Coupled Nozzle Erosion Characterization," AIAA 2011-5799, July 2011, $47^{th}$ AIAA/ASME/SAE/ASEE Joint Propulsion Conference and Exhibit, 31 July - 3 August 2011, San Diego, CA.

[17] Cavallini, E., Favini, B., Di Giacinto, M., and Serraglia, F., "SRM Internal Ballistic Numerical Simulation by SPINBALL Model," AIAA Paper 2009-5512, Aug. 2009, $45^{th}$ AIAA/ASME/SAE/ASEE Joint Propulsion Conference and Exhibit, Denver, Colorado.